Supplementary material

Hierarchical flower-like Ni-Co layered double hydroxide nanostructures: synthesis and super performance

Tao Dong [a], Xiao Zhang [b], Meng Li [a], Peng Wang[a], Ping Yang [a*]

a School of Material Science and Engineering, University of Jinan, Jinan 250022, China

b Fuels and Energy Technology Institute and Department of Chemical Engineering, Curtin University, Perth WA6845, Australia

*Corresponding Author has to be addressed.E-mail address: mse_yangp@ujn.edu.cn (P. Yang)

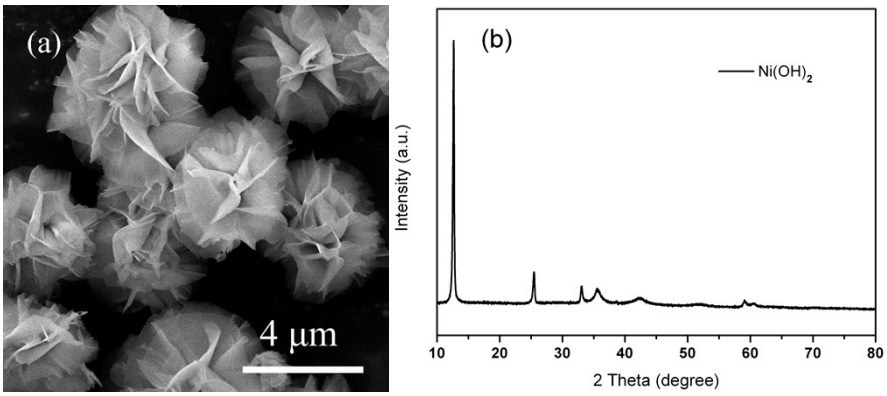

Fig. S1 (a) SEM image and (b) XRD pattern of $Ni(OH)_2$.

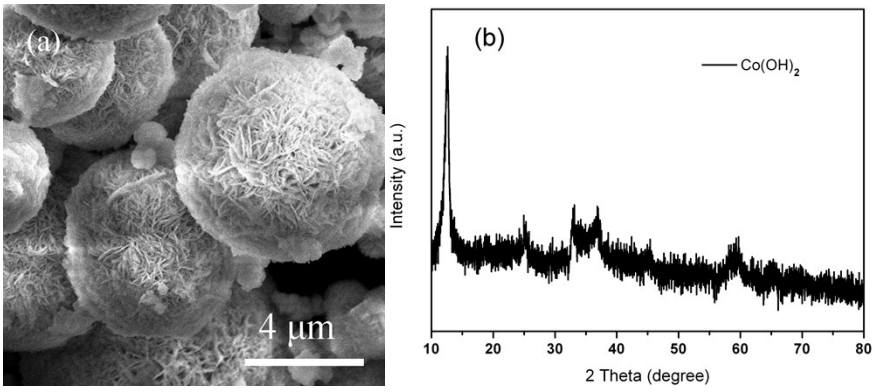

Fig. S2 (a) SEM image and (b) XRD pattern of $Co(OH)_2$.

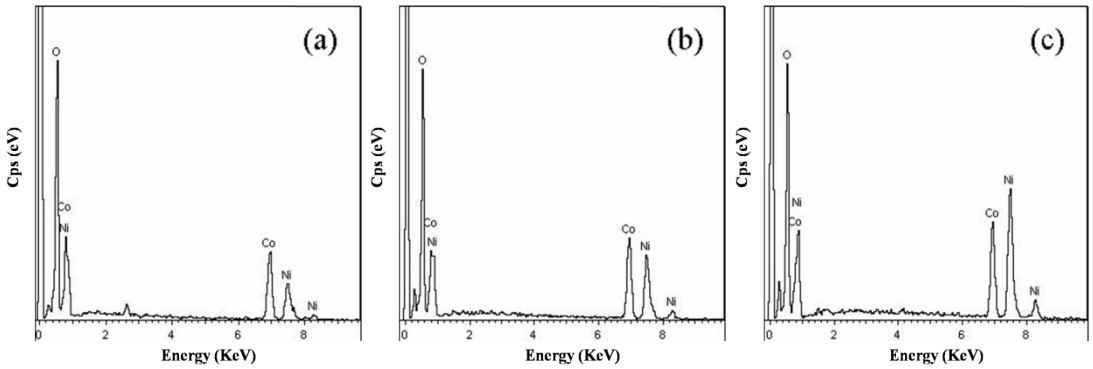

Fig. S3 EDS analysisof (a) Ni-Co LDH 1/2, (b) Ni-Co LDH 1/1 and (c) Ni-Co LDH 2/1.

Table S1 Atomic percentages of Ni, Co, and O elements.

Samples	Ni	Co	O
Ni-Co LDH 1/2	11.87	23.95	64.18
Ni-Co LDH 1/1	14.90	15.68	69.42
Ni-Co LDH 2/1	24.78	12.41	62.81

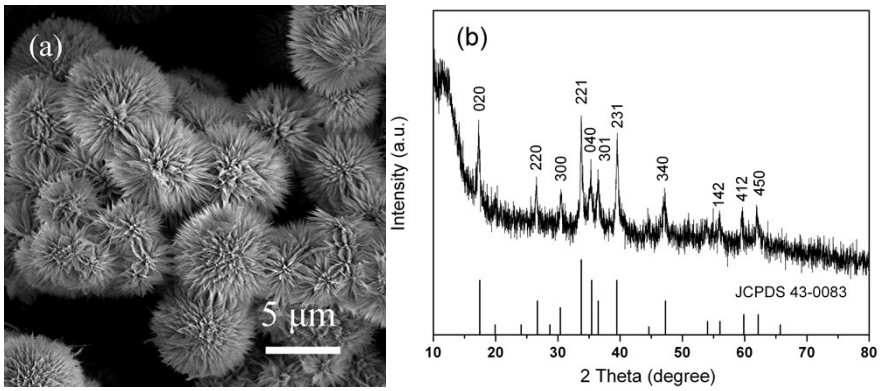

Fig. S4 (a) SEM image and (b) XRD pattern of product prepared with H_2O as the solvent.

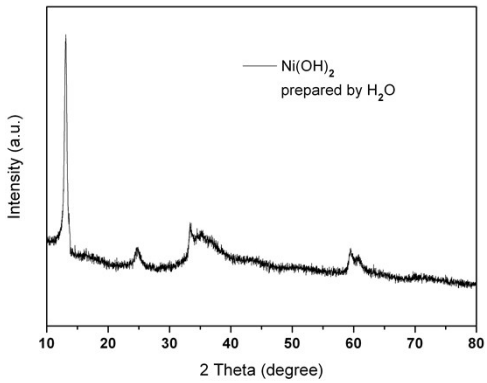

Fig. S5 XRD pattern of $Ni(OH)_2$ prepared with H_2O as the solvent.

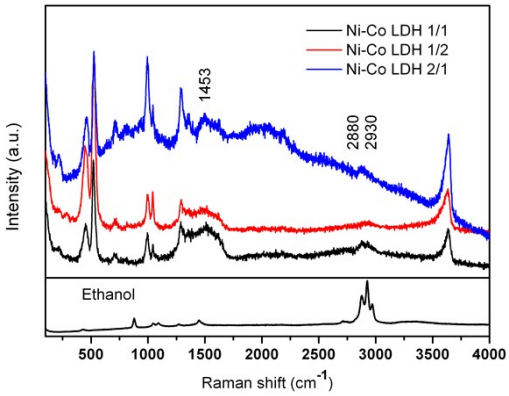

Fig. S6 Raman spectra of Ni-Co LDH 1/2, Ni-Co LDH 1/1, Ni-Co LDH 2/1 and ethanol.

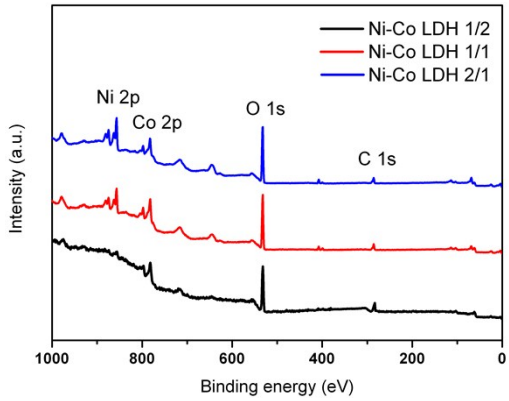

Fig. S7 XPS spectra of Ni-Co LDH 1/2, Ni-Co LDH 1/1 and Ni-Co LDH 2/1 for full survey scan.

Table S2. Kinetics models fitted data of AF adsorption with different adsorbents.

Sample	Pseudo first-order models				Pseudo second-order models		
	q_e (mg g^{-1}) experiment	q_e (mg g^{-1}) model	K_1	R^2	q_e (mg g^{-1}) model	K_2	R^2
Ni-Co LDH 1/2	230.5	243.3	1.04	0.92698	253.8	0.00303	0.99779
Ni-Co LDH 1/1	252.6	291.5	0.25	0.95621	275.5	0.0188	0.99772
Ni-Co LDH 2/1	211.1	231.5	1.81	0.99405	234.8	0.00223	0.99966
$Ni(OH)_2$	229.2	241.3	2.13	0.95499	236.4	0.00144	0.99275
$Co(OH)_2$	224.6	251.2	1.79	0.98102	243.9	0.00268	0.99926

Table S3. Kinetics models fitted data of CR adsorption with different adsorbents.

Sample	Pseudo first-order models				Pseudo second-order models		
	q_e (mg g^{-1}) experiment	q_e (mg g^{-1}) model	K_1	R^2	q_e (mg g^{-1}) model	K_2	R^2
Ni-Co LDH 1/2	173.4	183.8	3.86	0.97538	184.8	$1.3*10^{-2}$	0.99791
Ni-Co LDH 1/1	245.2	259.7	0.59	0.97401	261.1	$6.1*10^{-2}$	0.99839
Ni-Co LDH 2/1	148.5	184.5	8.24	0.97171	193.4	$5.1*10^{-3}$	0.99703
$Ni(OH)_2$	165.8	159.7	7.18	0.91864	172.4	$5.8*10^{-3}$	0.99291
$Co(OH)_2$	163.4	174.2	4.33	0.96964	174.8	$7.9*10^{-3}$	0.99987

Table S4. Adsorption models fitted data of AF and CR adsorption onto Ni-Co LDH 1/1.

Adsorption	Langmuir models				Freundlich models		
	K_L (L mg^{-1})	q_{max} (mg g^{-1})	R_L	R^2	K_F (L mg^{-1})	n	R^2
AF	0.037	2787	0.043-0.119	0.99486	812.4	5.01	0.88851
CR	0.0424	1915.7	0.038-0.106	0.99690	937.7	9.69	0.90211

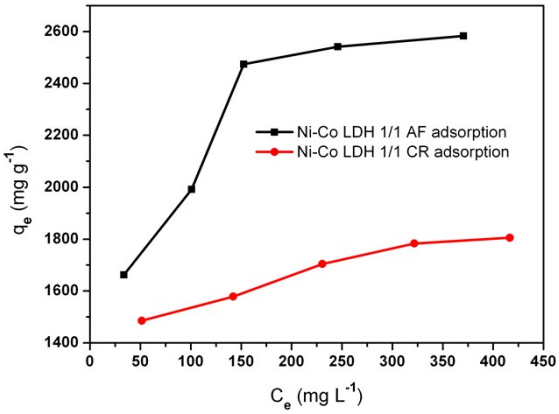

Fig. S8 Effect of dye concentrations on the equilibrium adsorption capacity of AF and CR adsorption onto Ni-Co LDH 1/1.

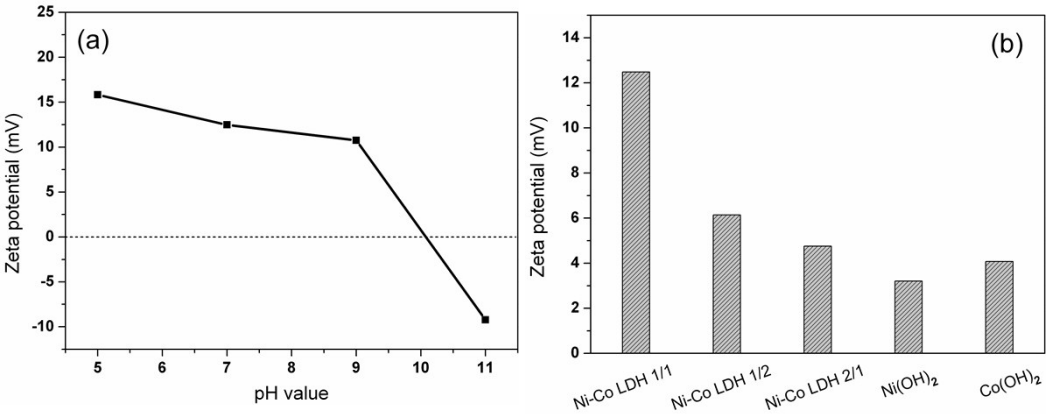

Fig. S9 (a) Zeta potential of Ni-Co LDH 1/1 at different pH values. (b) Zeta potential of Ni-Co LDH 1/1, Ni-Co LDH 1/2, Ni-Co LDH 2/1, $Ni(OH)_2$ and $Co(OH)_2$ at pH values of 7.

Table S5 Comparison of maximum adsorption capacitance for acid fuchsin of various adsorbents.

Adsorbents	q_{max} (mg g^{-1})	References
Ni-Co LDH 1/1	2787(AF) 1915.7 (CR)	This work
C/$NiFe_2O_4$	21(AF)	[1]
NiOnanosheets	22(AF)	[2]
Chitosan	43(AF)	[3]
Graphene oxide/chitosan	130(AF)	[4]
Montmorillonite	161(AF)	[5]
Carbon–alumina composite	95 (AF)	[6]
$ZnFe_2O_4$ hollow fibers	150(AF)	[7]
LTA-type zeolite	40(AF)	[8]
CLDH/γ-AlO(OH)-2-500	447 (CR)	[9]
MgO (111) nanoplates	303 (CR)	[10]
Activated carbon powder	500 (CR)	[11]
$CoFe_2O_4$	244.5 (CR)	[12]
Activated carbon from coal	189 (CR)	[13]

Table S6 Comparisons of the specific capacitances for Ni-Co LDHs based electrode materials in three-electrode system.

Ni-Co LDHs based electrodes	Specific capacitances(F g^{-1})	Ref.
Ni-Co LDH 1/2	3168.3 (1 A g^{-1})	This work
Ni-Co LDHs on conducting Zn_2SnO_4	1805 (0.5 A g^{-1})	[14]
Nickel/cobalt double hydroxides	1887.5 (1 A g^{-1})	[15]
Ni-Co LDH nanosheets	2682 (3 A g^{-1})	[16]
Vertically aligned Ni-Co LDHs nanosheet	1734 (6 A g^{-1})	[17]
Ni-Co LDHs nanoflakes/carbon cloth	1938 (1 A g^{-1})	[18]
Carbon nanotubes/Ni-Co hydroxide nanoflake	1151 (1 A g^{-1})	[19]
Flower-like nickel–cobalt binary hydroxides	1804 (1 A g^{-1})	[20]
Nitrogen-Doped Carbon Nanofiber/Ni-Co LDHs	1950 (1 A g^{-1})	[21]

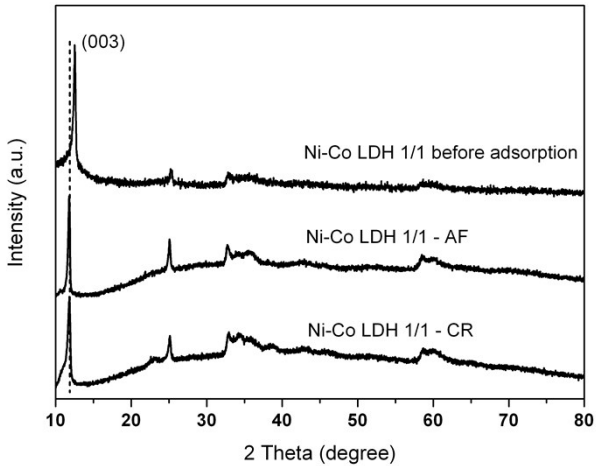

Fig. S10 XRD patterns of Ni-Co LDH 1/1 before and after AF and CR adsorption.

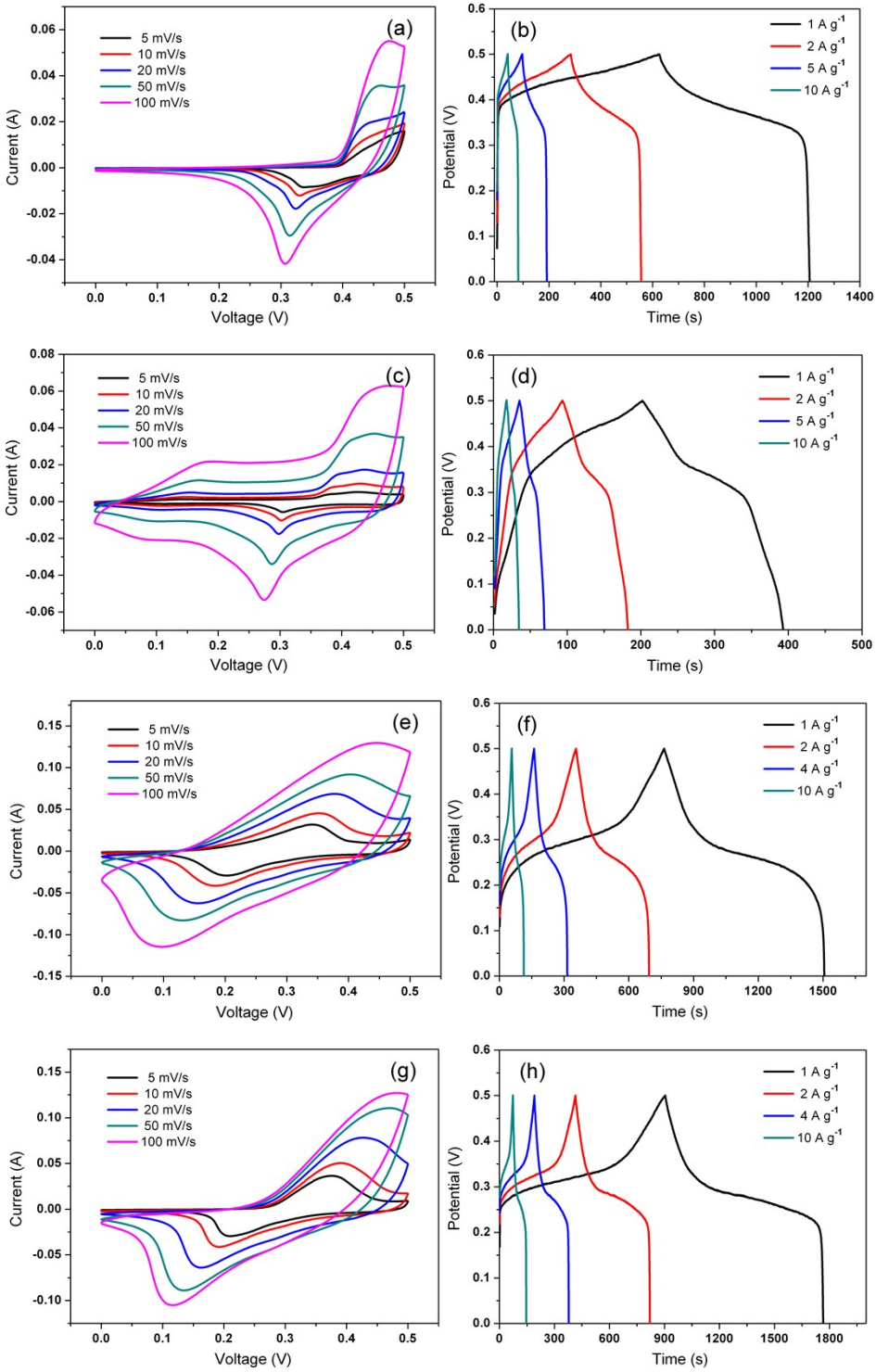

Fig. S11 CV and galvanostatic charge/discharge curves: (a) and (b) $Ni(OH)_2$ electrode, (c) and (d) $Co(OH)_2$ electrode, (e) and (f) Ni-Co LDH 1/1electrode and (g) and (h) Ni-Co LDH 2/1 electrode.

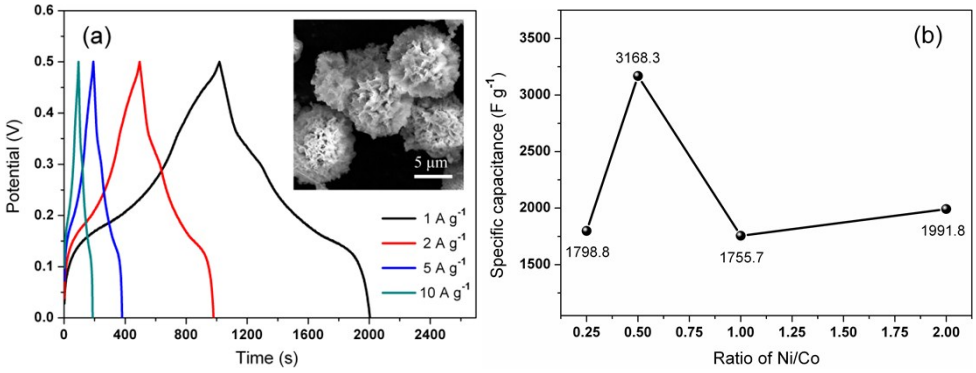

Fig. S12 (a) Galvanostatic charge/discharge curves of Ni-Co LDH with molar ratio of Ni/Co is 1:4, inset shows the SEM image. (b) Relationship plot between discharge specific capacitance and molar ratio of Ni/Co at current density of 1 A g^{-1}.

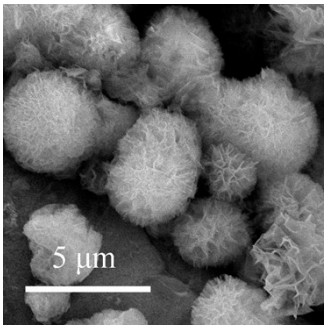

Fig. S13 SEM image of Ni-Co LDH 1/2 electrode after 3000 cycles.

The specific capacitances (SC) were calculated using the integral current areas of galvanostatic discharge curve with following formula [22]:

$$SC = \frac{2I_m \int V dt}{V_i^2 - V_f^2}$$

I_m (A g^{-1}) is the current density, where I is the current and m is the mass of active material. $\int V dt$ is the integral current area, where V is the potential with initial and final values of V_i and V_f, respectively. In this work, the area of the working electrode immersed into the electrolyte was controlled to be about 1 cm^2.

References

[1] X. Chen, Fine Chem. 30 (2013) 776–781.
[2] Z. Song, L. Chen, J. Hu, R. Richards, Nanotechnology 20 (2009) 275707.
[3] H. Jia, X. Wang, B. Han, Chin. J. Environ. Eng. 5 (2011) 1800–1805.
[4] A. Li, J. Sun, Q. Du, L. Zhang, X. Yang, S. Wu, Y. Xia, Z. Wang, Carbohydr. Polym. 102(2014) 755–761.
[5] A. S. Elsherbiny, Appl. Clay Sci. 83–84 (83) (2013) 56–60.

[6] M. Dutta, J.K. Basu, Int. J. Environ. Sci. Technol. 11 (2014) 87–96.
[7] J. Li, D.H.L. Ng, P. Song, Y. Song, C. Kong, J. Ind. Eng. Chem. 23 (2015) 290–298.
[8] H. Y. Xu, L. C. Wu, T. N. Shi, W. C. Liu, S. Y. Qi, Sci. China Technol. Sci. 57 (2014) 1127–1134.
[9] J. Lia, N. Zhang, D. H. L. Ng, J. Mater. Chem. A 3 (2015) 21106–21115.
[10] J. Hu, Z. Song, L. Chen, H. Yang, J. Li, R. Richards, J. Chem. Eng. Data 55 (2010) 3742–3748.
[11] M. Szlachta, P. Wójtowicz, Water Sci. Technol. 68 (2013) 2240–2248.
[12] L. Wang, J. Li, Y. Wang, L. Zhao, Q. Jiang, Chem. Eng. J. 181 (2012) 72–79.
[13] E. L. Grabowska, G. Gryglewicz, Dyes Pigments 74 (2007) 34–40.
[14] W. Xu, A. Sumboja, M. F. Lin, J. Yan, P. S. Lee, Nanoscale 4 (2012) 7266–7272.
[15] T. Yan, H. Y. Zhu, R. Y. Li, Z. J. Li, J. K. Liu, G. L. Wang, Z. Q. Gu, Electrochim. Acta 111 (2013) 71–79.
[16] H. Chen, L. F. Hu, M. Chen, Y. Yan, L. M. Wu, Adv. Funct. Mater. 24 (2014) 934.
[17] J. Pu, Y. Tong, S. B. Wang, E. H. Sheng, Z. H. Wang, J. Power Sources 250 (2014) 250–256.
[18] M. F. Warsi, I. Shakir, M. Shahid, M. Sarfraz, M. Nadeem, Z. A. Gilani, Electrochim. Acta 135 (2014) 513–518.
[19] M. Li, K. Y. Ma, J. P. Cheng, D. H. Lv, X. B. Zhang, J. Power Sources 286 (2015) 438–444.
[20] J. Zhang, J. P. Cheng, M. Li, L. Liu, F. Liu, X. B. Zhang, J. Electroanal. Chem.743 (2015) 38–45.
[21] F.L. Lai, Y.E. Miao, L.Z.Zuo, H.Y. Lu, Y.P. Huang,T.X. Liu, small 12 (2016) 3235–3244.
[22] L. Q. Mai, A. M. Khan, X. C. Tian, K. M. Hercule, Y. L. Zhao, X. Lin, X. Xu, Nat. Commun. 4 (2013) 2923 doi: 10.1038/ncomms3923.